A NEW PID CONTROLLER AUTO-TUNING METHOD BASED ON MULTIPLE INTEGRATIONS

Damir Vrančić

J. Stefan Institute, Jamova 39, SI-1001 Ljubljana, Slovenia
e-mail: damir.vrancic@ijs.si
home page: http://www-e2.ijs.si/People/Damir.Vrancic.html

Abstract: The magnitude optimum (MO) technique provides non-oscillatory closed-loop response for a large class of process models. However, this technique is based on an accurate model which requires precise process identification and extensive computations. In the present lecture, it is shown that there exists a close relation between multiple integrations of the process step response and the MO criterion. Thanks to this relation, the MO criterion can be achived in a very simple way. Some practical guidelines how to perform multiple integrations and how to re-tune controller parameters are given. A description of an auto-tuning algorithm, based on this new approach, with real-time examples on the laboratory set-ups is given as well.

Keywords: PI controllers, PID controllers, Moment method, Multiple integration, Magnitude optimum

1. INTRODUCTION

The Ziegler-Nichols tuning rules (Ziegler and Nichols, 1942) were the very first tuning rules for PID controllers, and it is surprising that they are still widely used today. The reason for their popularity lies in their simplicity and efficiency. This is why so many different tuning rules which are based on the same tuning procedures have been developed later on (Gorez, 1997).

After the work of Ziegler and Nichols, a variety of PID tuning methods have been developed. In general, these methods can be divided into two main groups: the *direct* and the *indirect* tuning methods (Åström et al., 1993; Gorez, 1997). The direct tuning methods do not require a process model, while the indirect methods calculate controller parameters from identified model of the process.

The purpose of this lecture is to introduce a new indirect tuning method which is based on an implicit process model rather than an explicit one. The *multiple integrations* method (Rake, 1987; Strejc, 1959) is used for the implicit process identification. However, the areas, calculated by using the multiple integrations from the open-loop process response, are directly used for the calculation of the controller parameters rather than for the process identification (Nishikawa et al., 1984; Voda and Landau, 1995) in order to meet the so-called *magnitude optimum* (MO) *criterion* (Åström and Hägglund, 1995; Hanus, 1975; Kessler, 1955; Umland and Safiuddin, 1990). It was found out that in this way the magnitude optimum criterion can be met for a very large set of process models (low-order, high-order, highly non-minimum phase and/or processes with larger time delays) merely by measuring the process open-loop step response without the need for additional "fine" tuning.

The lecture is organised as follows. Section 2 provides a theoretical background with derivation of PID controller parameters, according to the new magnitude optimum multiple integrations (MOMI) method. Next, in Section 3, some guidelines on how to perform the multiple integrations in practice and how to re-tune controller parameters are given. Real-time auto-tuning algorithm with experiments on two laboratory plants are given in Section 5. Some additional thoughts concerning the MO criterion and MOMI method are stated in Section 6. The lecture ends up with conclusions.

2. DERIVATION OF PID CONTROLLER PARAMETERS

The tuning procedure for the PID controller is given for processes which can be approximated by the transfer function

$$G_P(s) = K_{PR}\frac{1+b_1s+b_2s^2+\cdots+b_ms^m}{1+a_1s+a_2s^2+\cdots+a_ns^n}e^{-sT_{del}} \quad , \qquad (1)$$

where K_{PR} denotes the process steady-state gain, and a_1 to a_n and b_1 to b_m are the corresponding parameters ($m\leq n$) of the process transfer function, and T_{del} represents the process pure time delay.

The PID controller is given by the following transfer function:

$$G_C(s) = \frac{U(s)}{E(s)} = K\left(1+\frac{1}{sT_i}+\frac{sT_d}{1+sT_f}\right), \qquad (2)$$

where U and E denote the Laplace transforms of the controller output, and the control error ($e=w-y$), respectively. The controller parameters K, T_i, T_d, and T_f represent proportional gain, integral time constant, derivative time constant, and filter time constant, respectively.

The PID controller in a closed-loop configuration with the process is shown in Fig. 1, where d denotes a load disturbance.

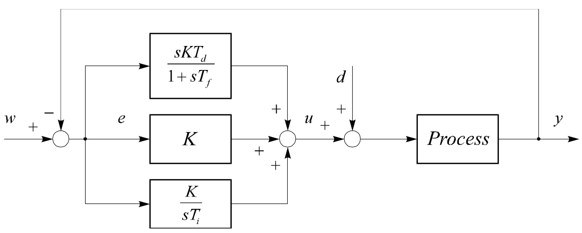

Fig. 1. The closed loop system with PID controller

The goal of tuning is to find such a controller that makes the closed-loop magnitude (amplitude) frequency response (G_{CL}) from the set-point to the plant output as flat and as close to unity as possible for a large bandwidth. The requirements can be expressed in the following way:

$$\left|G_{CL}(j\omega)\right| = \left|\frac{Y(j\omega)}{W(j\omega)}\right| = \left|\frac{G_P(j\omega)G_C(j\omega)}{1+G_P(j\omega)G_C(j\omega)}\right| \approx 1 \ . \qquad (3)$$

This technique is called magnitude optimum (MO) (Umland and Safiuddin, 1990), modulus optimum (Åström and Hägglund, 1995), or Betragsoptimum (Åström and Hägglund, 1995; Kessler, 1955), and results in a fast and non-oscillatory closed-loop time response for a large class of process models.

The closed-loop tuning goal can be easily transformed into the open-loop criterion by using the well-known M and N circles known from the basic control theory. To achieve the same tuning goal as given above, the open-loop Nyquist curve should follow the vertical line with the real value -0.5 up to the highest frequency possible (Hanus, 1975). If the controller is of the same order as the process, the open-loop Nyquist curve will follow the vertical line up to the frequency $\omega=\infty$ (see solid line in Fig. 2). Otherwise, open-loop Nyquist curve will turn away from the vertical line at higher frequencies (see dashed line in Fig. 2).

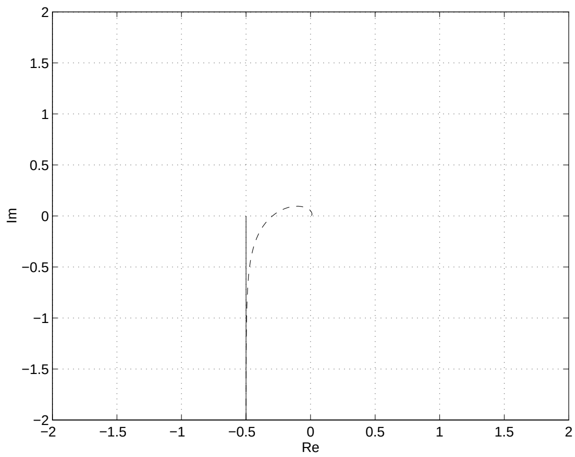

Fig. 2. Nyquist chart of the open-loop frequency response $G_P(j\omega)G_C(j\omega)$;
__ frequency response when using a controller with same order than the process,
-- frequency response when using a controller with lower-order than the process.

Following the procedure given by Hanus, (1975), such tuning goal can be achieved by moving the zeros of the function $\mathbf{Re}\{G_P(j\omega)G_C(j\omega)\}+0.5$ toward $\omega=0$.

In order to derive the PI and the PID controller parameters according to the given MO criterion, firstly the pure time delay in equation (1) has to be developed into the Taylor series:

$$e^{-sT_{del}} = 1 - sT_{del} + \frac{(sT_{del})^2}{2!} - \frac{(sT_{del})^3}{3!} + \cdots . \qquad (4)$$

The open-loop system transfer function can then be expressed in the following way:

$$G_C(s)G_P(s) = \frac{d_0+d_1s+d_2s^2+d_3s^3+\ldots}{c_0s+c_1s^2+c_2s^3+c_3s^4+\ldots}, \qquad (5)$$

where parameters c_i and d_i are functions of the transfer function (Equation 1), and PID controller (Equation 2) parameters (see e.g. Vrančić et al., 1997c).

In order to determine *three* PID controller parameters, as required by the presented magnitude optimum criterion, the first *three* equations (n=0..2) from the following set of equations must hold (Hanus, 1975):

$$\sum_{i=0}^{2n+1}(-1)^i d_i c_{2n+1-i} = \frac{1}{2}\sum_{i=0}^{2n}(-1)^i c_i c_{2n-i} \tag{6}$$

When inserting parameters c_i and d_i from equation (5) into equation (6), and applying T_f=0[1], the following PID controller parameters can be expressed by the unknown process parameters (Vrančić, 1997):

$$K = \frac{\begin{bmatrix} a_1^3 - a_1^2 b_1 + a_1 b_2 - 2a_1 a_2 + a_2 b_1 + \\ + a_3 - b_3 + T_{del}\left(a_1^2 - a_1 b_1 - a_2 + b_2\right) + \\ + \frac{T_{del}^2}{2}\left(a_1 - b_1\right) + \frac{T_{del}^3}{6} \end{bmatrix}}{2K_{PR}\begin{bmatrix} - a_1^2 b_1 + a_1 a_2 + a_1 b_1^2 - a_3 - b_1 b_2 + \\ + b_3 + T_{del}\left(a_1 - b_1\right)^2 + T_{del}^2\left(a_1 - b_1\right) + \\ + \frac{T_{del}^3}{3} - T_d\left(a_1 - b_1 + T_{del}\right)^2 \end{bmatrix}} \tag{7}$$

$$T_i = \frac{\begin{bmatrix} a_1^3 - a_1^2 b_1 + a_1 b_2 - 2a_1 a_2 + a_2 b_1 + \\ + a_3 - b_3 + T_{del}\left(a_1^2 - a_1 b_1 - a_2 + b_2\right) + \\ + \frac{T_{del}^2}{2}\left(a_1 - b_1\right) + \frac{T_{del}^3}{6} \end{bmatrix}}{\begin{bmatrix} a_1^2 - a_1 b_1 - a_2 + b_2 + T_{del}\left(a_1 - b_1\right) + \frac{T_{del}^2}{2} - \\ - T_d\left(a_1 - b_1 + T_{del}\right) \end{bmatrix}} \tag{8}$$

$$T_d = f\left(a_1 \cdots a_5, b_1 \cdots b_5, T_{del}\right) \tag{9}$$

Note that the explicit result for the derivative time constant is not given. The reason is that equation (9) would fill up one full page of this lecture.

In order for the method to be applied, an explicit identification of the parameters K_{PR}, a_1, a_2, a_3, a_4, a_5, b_1, b_2, b_3, b_4, b_5, and T_{del} of the transfer function (Equation 1) is required. However, it is well known that exact and reliable identification of such a number of parameters from real measurements is very problematic.

This problem can be avoided by using the concept of multiple integrations (Rake, 1987; Strejc, 1959). Following Rake, (1987), and considering equation (1), the following areas can be expressed by integrating the process open-loop step response ($y(t)$), after applying the step-change ΔU at the process input:

$$\begin{aligned} A_1 &= y_1(\infty) = K_{PR}\left(a_1 - b_1 + T_{del}\right) \\ A_2 &= y_2(\infty) = K_{PR}\left[b_2 - a_2 - T_{del}b_1 + \frac{T_{del}^2}{2!}\right] + \\ &\quad + A_1 a_1 \\ &\vdots \\ A_k &= y_k(\infty) = K_{PR}\begin{pmatrix} (-1)^{k+1}\left(a_k - b_k\right) + \\ + \sum_{i=1}^{k}(-1)^{k+i}\frac{T_{del}^i b_{k-i}}{i!} \end{pmatrix} + \\ &\quad + \sum_{i=1}^{k-1}(-1)^{k+i-1}A_i a_{k-i} \end{aligned} \tag{10}$$

where

$$\begin{aligned} y_0(t) &= \frac{y(t) - y(0)}{\Delta U} \\ y_1(t) &= \int_0^t \left[K_{PR} - y_0(\tau)\right]d\tau \quad , \\ &\vdots \\ y_k(t) &= \int_0^t \left[A_{k-1} - y_{k-1}(\tau)\right]d\tau \end{aligned} \tag{11}$$

In order to clarify the mathematical derivation, graphic representations of the first three areas (A_1 to A_3) are shown in Figures 3 to 5.

When inserting the calculated areas (Equation 10), obtained from the process open-loop step response, into equations (7) to (9), the following result is obtained:

$$T_d = \frac{A_3 A_4 - A_2 A_5}{A_3^2 - A_1 A_5} \tag{12}$$

$$K = \frac{A_3}{2\left(A_1 A_2 - A_3 K_{PR} - T_d A_1^2\right)} \tag{13}$$

$$T_i = \frac{A_3}{A_2 - T_d A_1} \tag{14}$$

Note that the PI controller parameters can be expressed from equations (13) and (14) simply by applying T_d=0.

[1] The derivation of PID controller parameters, when $T_f \neq 0$ is given in Vrančić (1997). However, T_f does not affect seriously the accuracy of the calculated controller parameters when choosing $T_f = T_d/10$ as was used in all the closed-loop experiments given in this lecture.

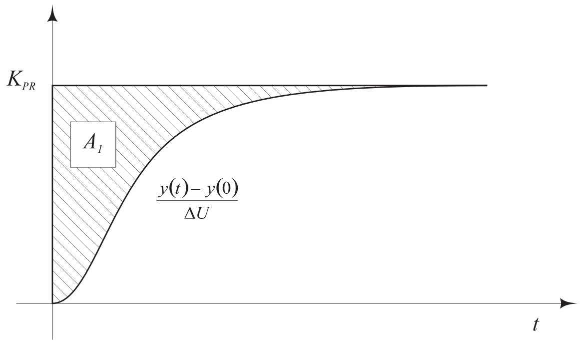

Fig. 3. The graphic representation of area A_1

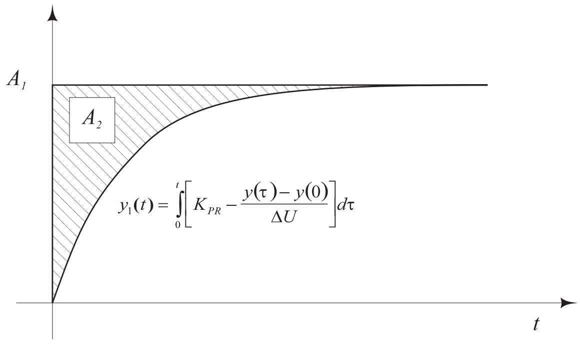

Fig. 4. The graphic representation of area A_2

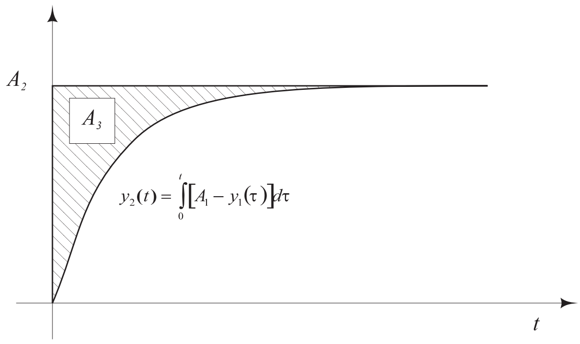

Fig. 5. The graphic representation of area A_3

Now obviously only the process steady-state gain K_{PR}, and five areas (A_1 to A_5) are needed to calculate the unknown PID controller parameters, and three areas (A_1 to A_3) to calculate the unknown PI controller parameters.

As seen from equations (10) and (11), or Figures 3 to 5, the areas A_1 to A_5 can be calculated from the process open-loop step response by a simple numerical integration, whilst the gain K_{PR} can be determined from the steady-state value of the process step response in the usual way.

All together this means substantial reduction of the number of the required parameters (areas A_1 to A_5 instead of transfer function parameters $a_1..a_5$, $b_1..b_5$, and T_{del}) and consequently important simplification of expressions for K, T_i, and T_d.

One of the main points is, however, that the mapping of equations (7), (8), and (9) into equations (13), (14), and (12) is an exact and not an approximate one. This means that the PID parameters defined by the MO criterion and originally expressed by complicated relations between the parameters of the transfer function, can be equally well expressed by single combination of corresponding areas obtained from the step response.

The PID controller tuning procedure can therefore proceed as follows:

- measure the process step response,
- find the process steady-state gain K_{PR} and areas A_1, to A_5 (by using numerical integration (summation) from the start to the end of the process step response), and
- calculate the PID controller parameters by using equations (12) to (14).

2.1 *Illustrative example*

Let us now illustrate the proposed PID controller design in one example.

The following fifth-order process model is chosen:

$$G_P(s)=\frac{1.5}{(1+s)^5} \quad . \tag{15}$$

At first, a step-change ΔU=2 is applied to the process input. The process open-loop step response is shown in Fig. 6 above. The starting process steady-state is $y(0)=0$, and the final steady-state of the process is $y(\infty)=3$, so the process steady-state gain $K_{PR}=(y(\infty)-y(0))/\Delta U=1.5$. Function $y_1(t)$ is obtained by numerically integrating a difference $K_{PR}-(y(t)-y(0))/\Delta U$, as given by equation (11). Function $y_1(t)$ is shown in Fig. 6 below. The final steady-state $y_1(\infty)=7.5$ equals area A_1 (10). Similarly, area A_2 can be obtained by numerically integrating the difference between $A_1=y_1(\infty)$ and $y_1(t)$, as given by equations (10) and (11). Calculated function $y_2(t)$ is given in Fig. 7. The final steady-state value of $y_2(t)$ corresponds to A_2 ($A_2=y_2(\infty)=22.5$). The remaining functions (y_3 to y_5) and areas (A_3 to A_5) can be calculated in the similar manner. Functions $y_3(t)$ to $y_5(t)$ are shown in Fig. 7.

Hence, the following values of the process steady-state gain and the areas are obtained from the process step-response:

$$\begin{aligned} &K_{PR}=1.5,\ \ A_1=7.5,\ \ A_2=22.5,\\ &A_3=52.5,\ \ A_4=105,\ \ A_5=189 \end{aligned} \quad . \tag{16}$$

The optimal PID controller parameters are calculated from equation (16) by using equations (12) to (14):

$$K=0.708,\ \ T_i=3.4s,\ \ T_d=0.94s \quad . \tag{17}$$

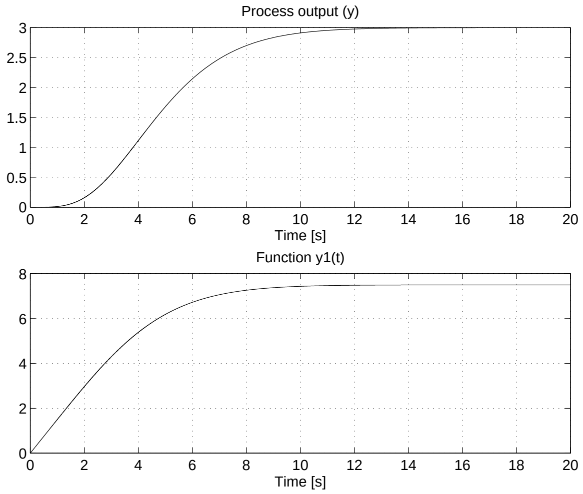

Fig. 6. Process step response (y) (above) and function $y_1(t)$ (below)

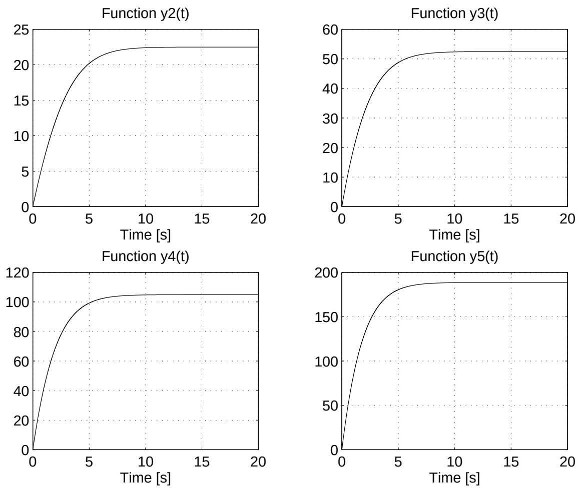

Fig. 7. Function $y_2(t)$ (above left), function $y_4(t)$ (above right) , function $y_5(t)$ (below left), and function $y_5(t)$ (below right)

The optimal PI controller parameters can be calculated as well by applying T_d=0 into equations (13) and (14):

$$K = 0.292, \quad T_i = 2.33s \ . \tag{18}$$

Fig. 8 shows the closed-loop time responses on the reference change (w=1 at t=0s), and on the load-disturbance (d=1 at t=30s) when using the PI and the PID controller. It is clear that both closed-loop responses are quite acceptable, all according to the chosen MO tuning criterion.

Two Nyquist curves of the open-loop frequency response $G_C(j\omega)G_P(j\omega)$ (when using the PI and the PID controller) are shown in Fig. 9. It is clear that both Nyquist curves closely follow the vertical line with the real value -0.5 at lower frequencies, as prescribed by the MO tuning criterion.

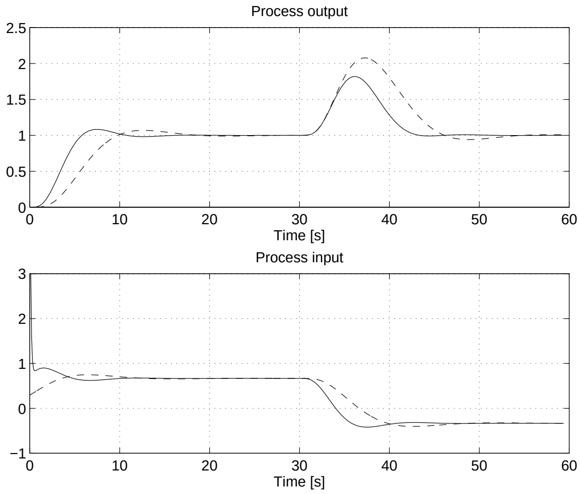

Fig. 8. Process output (y) (above) and controller output (u) (below) during the closed-loop experiment with: __ PID controller, -- PI controller

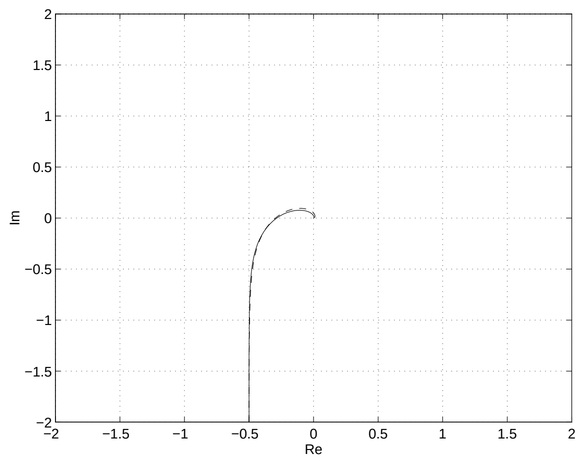

Fig. 9. Nyquist curve of the open-loop frequency response when using: __ PID controller, -- PI controller

3. SOME GUIDELINES FOR PRACTICAL WORK

In the previous section it was shown that the implementation of the magnitude optimum multiple integrations (MOMI) method is very simple and straightforward. Only the process step response has to be measured and some integrations (summations) to be performed in order to calculate areas A_1 to A_5 (A_1 to A_3 for PI controller). However, there are always some additional obstacles which have to be overcome in order to be able to implement the method in practice. In this section a few practical guidelines for deriving areas from process step response will be given, as well as some modifications of the tuning procedure if the calculated controller gain is too high or even negative.

3.1 Performing multiple integrations in practice

Areas A_1 to A_5 can be calculated from the final values (t=∞) of signals y_1(t) to y_5(t) (Equation 10). In practice, of course, it is enough to wait until process step response settles. Fig. 10 shows a typical process step response. At $t=t_1$, a step-change is applied to the process input. Process practically reaches the steady-state value at $t=t_{int}$, so all integrations in equation (11) can be made in time interval $t=[t_1, t_{int}]$.

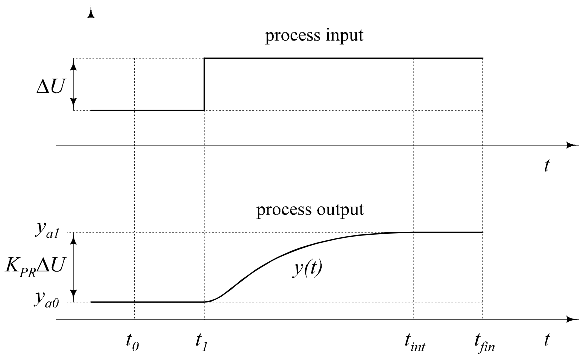

Fig. 10. Process input and output during step-change experiment.

However, making relatively small errors in the calculation of the process steady-state gain (K_{PR}) could lead to relatively large errors in calculated areas. Such errors are especially noticeable when dealing with process with present noise. In order to improve the accuracy of the calculated K_{PR}, the process step response should be averaged in time intervals
$t=[t_0, t_1]$ (before making step change) and $t=[t_{int}, t_{fin}]$ (after new steady-state is already achieved) in the following way (see Fig. 10):

$$\begin{aligned} y_{a0} &= \overline{y(t)};\;\; t = [t_0,\, t_1] \\ y_{a1} &= \overline{y(t)};\;\; t = [t_{\mathbf{int}},\, t_{fin}] \end{aligned} \tag{19}$$

A process steady-state gain is then simply calculated as:

$$K_{PR} = \frac{y_{a1} - y_{a0}}{\Delta U} \tag{20}$$

Note that $y(0)$ in (11) should be replaced by y_{a0}.

How to choose time instants t_0 and t_{fin}? Numerous experiments on several process models and laboratory plants showed that good practical results are usually obtained when choosing:

$$\begin{aligned} t_1 - t_0 &= 0.1 \ldots\; 0.3 \cdot (t_{int} - t_1) \\ t_{fin} - t_{int} &= 0.1 \ldots\; 0.3(t_{int} - t_1) \end{aligned} \tag{21}$$

Let us now illustrate the proposed integration procedure in one example.

The following process model is chosen:

$$G_P(s) = \frac{1}{(1+4s)^3}\;\; . \tag{22}$$

A random noise, generated by MATLAB function RANDN, and amplified by factor 0.05, was added to the process step response. The process output and input signals are shown in Fig. 11.

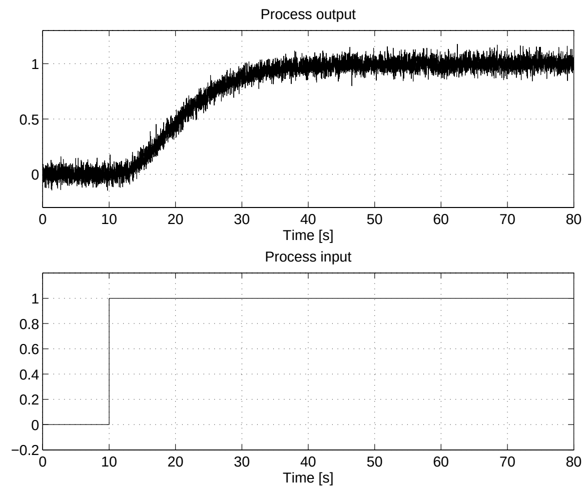

Fig. 11. Process output (y) and controller output (u) during the open-loop experiment on the process with present noise.

The following time intervals were chosen: t_0=0s, t_1=10s, t_{int}=50s, and t_{fin}=60s. Values y_{a0} and y_{a1} were calculated by averaging process output signal during intervals $t=[t_0, t_1]$ and $t=[t_{int}, t_{fin}]$ (Equation 19) and resulted in $y_{a0}=-6.97\cdot10^{-4}$, and $y_{a1}=0.996$. Using equation (20), the calculated process gain was $K_{PR}=0.997$. Functions y_1(t) to y_5(t) were calculated from equation (11), where integrations were performed in time interval $t=[t_1, t_{int}]$. Areas A_1 to A_5 were calculated from $y_1(t_{int})$ to $y_5(t_{int})$. The following values of areas and controller parameters were obtained:

$$\begin{aligned} &\mathit{process}\textbf{:}\;\; K_{PR} = 0.997,\;\; A_1 = 11.87, \\ &A_2 = 93.47,\;\; A_3 = 604.1,\;\; A_4 = 3433, \\ &A_5 = 1.762\cdot 10^4 \qquad\qquad . \\ &\mathit{PI}\textbf{:}\;\; K = 0.595,\;\; T_{\mathrm{i}} = 6.46 \\ &\mathit{PID}\textbf{:}\;\; K = 2.50,\;\; T_{\mathrm{i}} = 9.92,\;\; T_{\mathrm{d}} = 2.74 \end{aligned} \tag{23}$$

The ideal values, obtained on the process without present noise, were the following:

$$\begin{array}{l} process\text{:}\ K_{PR}=1,\ A_1=12,\ A_2=96, \\ A_3=640,\ A_4=3840,\ A_5=2.15\cdot 10^4 \\ PI\text{:}\ K=0.625,\ T_\mathrm{i}=6.67 \\ PID\text{:}\ K=2.31,\ T_\mathrm{i}=9.87,\ T_\mathrm{d}=2.59 \end{array} . \tag{24}$$

It is clear that the obtained controller parameters (Equation (23)) are close to the ideal ones (Equation (24)).

Tuning procedure, shown above, was used as a basis of the auto-tuning algorithm, which will be explained in more details in section 4.1.

3.2 Re-tuning the controller parameters

In some cases, the controller parameters, obtained by using the MOMI method, have to be re-tuned due to some practical reasons. Namely, when tuning the PID controllers for a first-order or second-order process the controller gain is in accordance with MO tuning criterion theoretically infinite. In practice (when process noise is present), the calculated controller gain can have a very high positive or negative value. In this case the controller gain should be limited to some acceptable value, which depends on the controller and the process limitations.

The remaining two controller parameters can now be calculated according to the limited (fixed) controller gain from equations (13) and (14):

$$T_i=\frac{A_1}{K_{PR}+\dfrac{1}{2K}} \tag{25}$$

and

$$T_d=\frac{A_3}{A_1^2}\left[\frac{A_1A_2}{A_3}-\frac{1}{2K}-K_{PR}\right] \tag{26}$$

if

$$K>\frac{1}{\dfrac{2A_1A_2}{A_3}-2K_{PR}} \tag{27}$$

and

$$T_d=0 \tag{28}$$

if

$$K\le\frac{1}{\dfrac{2A_1A_2}{A_3}-2K_{PR}} \tag{29}$$

When limiting the controller gain in the PI controller than, of course only equation (25) is used. Note that the proposed re-tuning of controller parameters can also be used in cases when slower and more robust controller should be designed (by decreasing the calculated gain K) or faster, but more oscillatory response is required (by increasing the calculated gain K).

Let us now illustrate the proposed modified tuning procedure.

The following process model is chosen:

$$G_P(s)=\frac{2}{(1+5s)(1+s)} . \tag{30}$$

The multiple integrations were performed on the process step response (y), and the following values of the process steady-state gain and areas were obtained from equations (10) and (11):

$$\begin{array}{l} K_{PR}=2,\ A_1=12,\ A_2=62, \\ A_3=312,\ A_4=1562,\ A_5=7812 \end{array} \tag{31}$$

In the next step PI and the PID controller parameters were calculated from equations (12) to (14):

$$\begin{array}{l} PI\text{:}\ K=1.3,\ T_i=5.03s \\ PID\text{:}\ K=\infty,\ T_i=6s,\ T_d=0.833s \end{array} \tag{32}$$

By fixing the controller gain to K=10, and by using equations (25) and (26), the following modified PID controller parameters were obtained:

$$K=10,\ T_i=5.85s,\ T_d=0.725s \tag{33}$$

Fig. 12 shows the process closed-loop responses when using the original PI controller and the modified PID controller parameters. It is clear that the process closed-loop response when using such modified PID controller is very good. The Nyquist curves of the open-loop system, when using the PI and the modified PID controller parameters, are shown in Fig. 13.

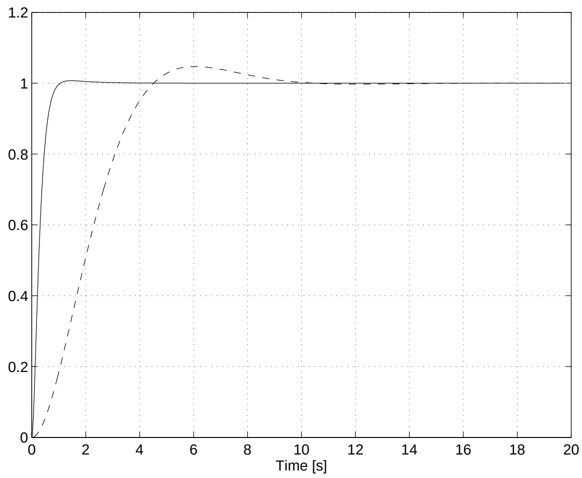

Fig. 12. Process output (y) and controller output (u) during the closed-loop experiment with: __ modified PID controller, -- PI controller

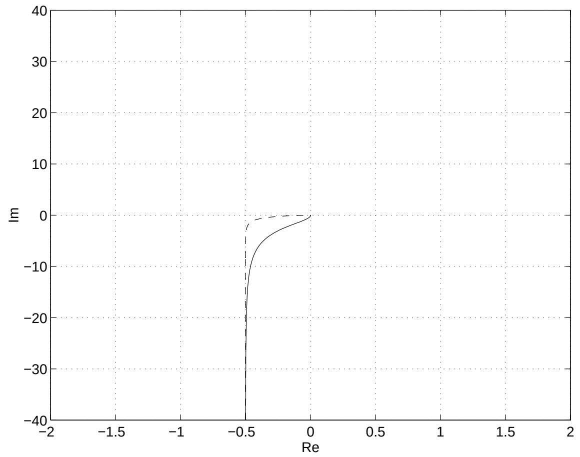

Fig. 13. Nyquist curves of the open-loop frequency response when using:
__ modified PID controller, -- PI controller

4. EXPERIMENTS ON LABORATORY PLANTS

4.1 Description of auto-tuning algorithm

An auto-tuning algorithm, made in the Pascal programme language has been built up to show the advantages of using the proposed tuning method in the auto-tuning controllers (Vrančić, 1997).

The block scheme of the auto-tuning algorithm is given in Fig. 14.

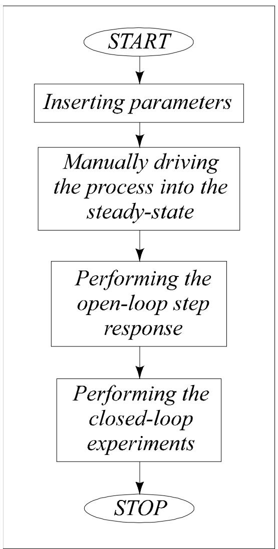

Fig. 14. Block diagram of the auto-tuning algorithm

4.1.1 Inserting parameters

At first, the algorithm requires some parameters for proper initialisation:

- sampling time (T_S),
- amplitude of the step-change at the process input (ΔU),
- maximum allowable proportional gain of the controller (K), (see sub-section 3.2), and
- approximate process main time constant (T_{main}).

The last parameter (T_{main}) does not have to be accurate. It is generally enough to estimate the range of the value (e.g. 1s, 10s, 100s...).

4.1.2 Manually driving the process into the steady-state

After inserting the parameters, the algorithm switches into the manual mode and the process has to be driven to the desired steady-state. When the process output settles the open-loop step-response can be performed.

4.1.3 Performing the open-loop step response

At first, a standard deviation (σ_1) and a mean value ($\bar{y}_1$) of the process output signal is measured by using the recursive algorithms, during the period $0<t\leq t_1=T_{main}/4$ (see Fig. 15 and a block-diagram in Fig. 16). Then, at $t=t_1=T_{main}/4$, a step-change ΔU is applied to the process input. After $t=t_1$, five integrals of $y(t)-\bar{y}_1$ are calculated recursively, where $y(t)$ denotes the process output and

$$\bar{y}_i = \frac{1}{t_i - t_{i-1}} \int_{t_{i-1}}^{t_i} y(t)dt = \overline{y(t)}; \quad t = [t_{i-1}, t_i]. \qquad (34)$$

Time instants t_1 to t_n are defined in the following way:

$$t_{i+1} = \begin{cases} t_i + \dfrac{T_{main}}{4} & ; \; t_i < T_{main} \\ 1.25 \cdot t_i & ; \; t_i \geq T_{main} \end{cases}. \qquad (35)$$

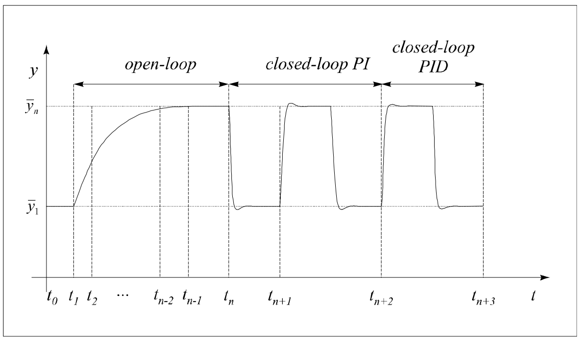

Fig. 15. Process output during the open-loop and the closed-loop experiments performed by the auto-tuning algorithm

In time intervals $t_{i-1} \le t \le t_i$ $(i=2...n)$, the process standard deviation:

$$\sigma_i = \frac{1}{t_i - t_{i-1}} \int_{t_{i-1}}^{t_i} \left(y(t) - \bar{y}_i \right) dt \qquad (36)$$

and the process mean value $\bar{y}_i$ (see Equation (34)) are recursively calculated. The multiple integrations of the process step response are also recursively calculated from $t=t_1$ and are terminated at $t=t_{n-1}$, when the standard deviation becomes $\sigma_{n-1} \le 2 \cdot \sigma_1$ or when $\sigma_{n-1} \le \sigma_{max}/40$, where

$$\sigma_{\max} = \max_{k=1\ldots n-1} \sigma_k \ . \qquad (37)$$

The steady-state gain of the process is calculated at $t=t_n$ in the following way:

$$K_{PR} = \frac{\bar{y}_n - \bar{y}_1}{\Delta U} , \qquad (38)$$

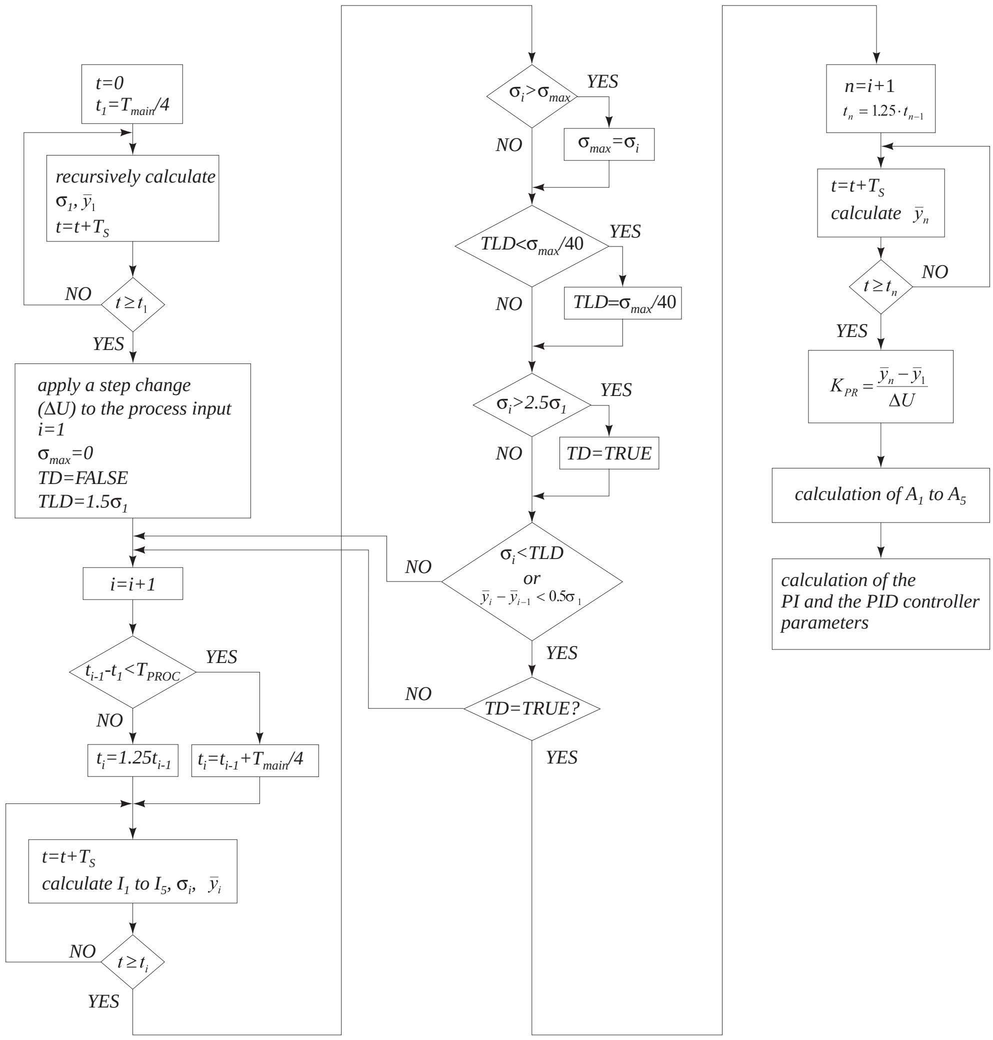

Fig. 16. Block-diagram of the auto-tuning algorithm whilst performing the open-loop step response.

At the same instant, the areas A_1 to A_5 are calculated:

$$A_1 = K_{PR}\left(t_{n-1} - t_1\right) - \frac{I_1}{\Delta U} , \qquad (39)$$

$$A_2 = A_1\left(t_{n-1} - t_1\right) - K_{PR}\frac{\left(t_{n-1} - t_1\right)^2}{2} + \frac{I_2}{\Delta U} , \qquad (40)$$

$$A_3 = A_2\left(t_{n-1} - t_1\right) - A_1\frac{\left(t_{n-1} - t_1\right)^2}{2} + K_{PR}\frac{\left(t_{n-1} - t_1\right)^3}{6} - \frac{I_3}{\Delta U} , \qquad (41)$$

$$A_4 = A_3\left(t_{n-1} - t_1\right) - A_2 \frac{\left(t_{n-1} - t_1\right)^2}{2} + A_1 \frac{\left(t_{n-1} - t_1\right)^3}{6} - K_{PR} \frac{\left(t_{n-1} - t_1\right)^4}{24} + \frac{I_4}{\Delta U}, \quad (42)$$

$$A_5 = A_4\left(t_{n-1} - t_1\right) - A_3 \frac{\left(t_{n-1} - t_1\right)^2}{2} + A_2 \frac{\left(t_{n-1} - t_1\right)^3}{6} - A_1 \frac{\left(t_{n-1} - t_1\right)^4}{24} + K_{PR} \frac{\left(t_{n-1} - t_1\right)^5}{120} - \frac{I_5}{\Delta U}, \quad (43)$$

where I_1 to I_5 are recursively calculated multiple integrations of the process step response:

$$I_1 = \int_{t_1}^{t_{n-1}} \left(y(\tau) - \bar{y}_1\right) d\tau, \quad (44)$$

$$I_2 = \int_{t_1}^{t_{n-1}} \left[\int_{t_1}^{\tau_1} \left(y(\tau) - \bar{y}_1\right) d\tau \right] d\tau_1, \quad (45)$$

$$I_3 = \int_{t_1}^{t_{n-1}} \left[\int_{t_1}^{\tau_3} \left[\int_{t_1}^{\tau_2} \left(y(\tau_1) - \bar{y}_1\right) d\tau_1 \right] d\tau_2 \right] d\tau_3, \quad (46)$$

$$I_4 = \int_{t_1}^{t_{n-1}} \left[\int_{t_1}^{\tau_4} \left[\int_{t_1}^{\tau_3} \left[\int_{t_1}^{\tau_2} \left(y(\tau_1) - \bar{y}_1\right) d\tau_1 \right] d\tau_2 \right] d\tau_3 \right] d\tau_4, \quad (47)$$

$$I_5 = \int_{t_1}^{t_{n-1}} \left[\int_{t_1}^{\tau_5} \left[\int_{t_1}^{\tau_4} \left[\int_{t_1}^{\tau_3} \left[\int_{t_1}^{\tau_2} \left(y(\tau_1) - \bar{y}_1\right) d\tau_1 \right] d\tau_2 \right] d\tau_3 \right] d\tau_4 \right] d\tau_5, \quad (48)$$

where the process step response $y(t)$ is approximated by the linear function between two samples:

$$y(t) = y(k-1) + \frac{y(k) - y(k-1)}{T_S}\left(t - t(k-1)\right); \quad t(k-1) < t \le t(k), \quad (49)$$

as given in Fig. 17.

After the process steady-state gain K_{PR} and areas A_1 to A_5 are obtained, the PI and the PID controller parameters are derived from expressions (12) to (14).

In order to achieve more robust auto-tuning algorithm, the proportional gain of the PID controller (K_{PID}) is additionally limited to four times the proportional gain of the PI controller (K_{PI}):

$$K_{PID} \le 4K_{PI}. \quad (50)$$

The remaining two PID controller parameters can be calculated from Equations (25) to (29).

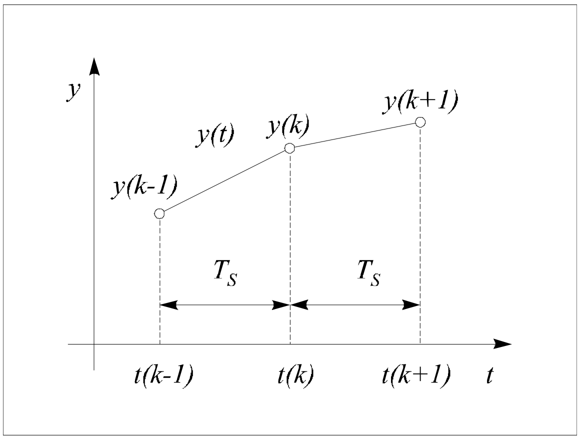

Fig. 17. The continuous-time approximation of the process step-response between two discrete samples.

4.1.4 Performing closed-loop experiments

After calculating areas A_1 to A_5, the PI and the PID controller parameters (the calculation is very fast due to the recursive way of numerical integration), the algorithm switches into automatic mode (into closed-loop configuration).

After switching to automatic mode, the reference step changes are applied (only for testing purposes), first by using the PI controller from $t_n<t\le t_{n+2}$, and then by using the PID controller from $t_{n+2}<t\le t_{n+3}$.

Note that in practical realisation of the PID controllers, the implementation of the appropriate anti-windup protection is of high importance. In this auto-tuning algorithm, the conditioning technique is applied as an anti-windup protection (see Peng et al., 1996).

4.2 Real-time experiments

Two real-time experiments were performed on the laboratory set-ups by using the Burr-Brown acquisition system PCI-20000 (Vrančić, 1997). The first experiment was made on a pneumatic set-up (process), given by Fig. 18. The input of the process is the current reference i_{in} (4/20 mA) on the servo-driven valve V_1 and the output is the pressure p_1 between valves V_1 and V_2 (transferred to the voltage u_{out} by using the pressure-to-voltage transmitter in the range from 0 to 10V).

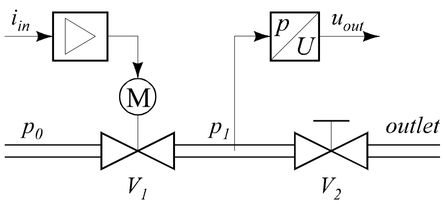

Fig. 18. Pneumatic set-up.

Fig. 19 shows the system time response when running the auto-tuning algorithm.

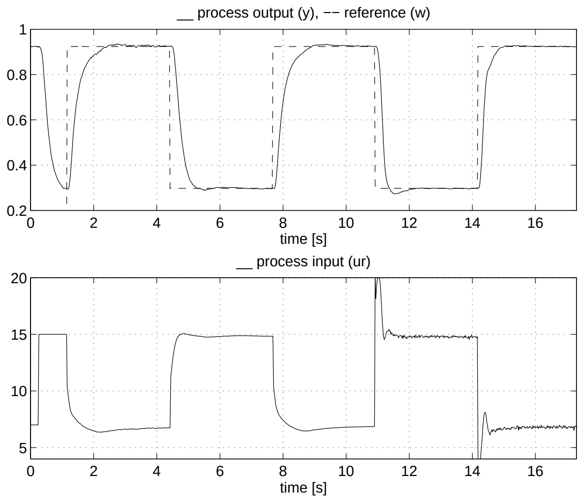

Fig. 19. Process output (upper Figure) and input (lower Figure) during the open-loop tuning period (0-1.2s) and the closed-loop testing period (1.2s-17s) of the auto-tuning algorithm.

Fig. 20 shows the process open-loop step response in more details from which the following values of the process gain K_{PR}, and areas A_1 to A_5 were calculated by the auto-tuning algorithm: K_{PR}=-0.0782, A_1=-0.0248, A_2=-4.919·10^{-3}, A_3=-7.746·10^{-4}, A_4=-1.039·10^{-4}, A_5=-1.219·10^{-5}.

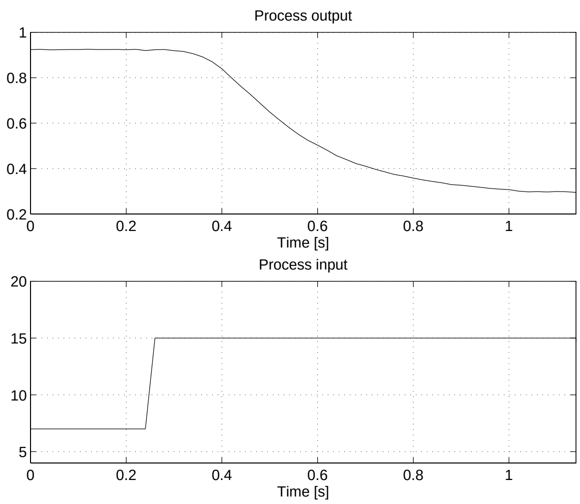

Fig. 20. The pneumatic set-up open-loop step response.

The corresponding PI and PID controller parameters are obtained from equations (12) to (14) and are:

$$\begin{aligned} &PI\text{:}\;\; K = -6.31,\; T_i = 0.157s \\ &PID\text{:}\;\; K = -20.36,\; T_i = 0.241s,\; T_d = 0.069s \end{aligned} \quad . \tag{51}$$

The closed-loop responses (see Fig. 21) are quite good for both controllers. It is obvious that the closed-loop time response is faster when using the PID controller, without significant increase of the process overshoot. Different closed-loop transients at low and high reference levels indicate the non-linear characteristics of the plant. The higher process time delay is clearly noticeable when decreasing the pressure, rather than when increasing the pressure (see Fig. 21).

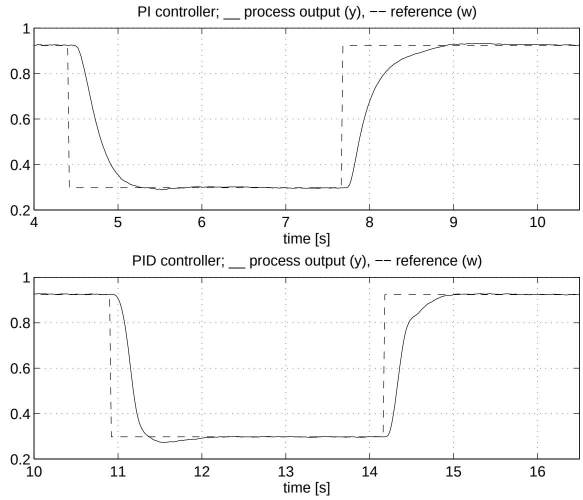

Fig. 21. The closed-loop process responses under PI and PID controller for the pneumatic set-up.

The second experiment was made on a motor-generator laboratory plant, as shown in Fig. 22.

The plant input is the voltage on the amplifier input (u_{in}) which drives the motor, and the output is the speed of the motor-generator system, measured at the output of the speed-to-voltage converter (u_{out}). Both input and output signals are in the range from 0 to 10V.

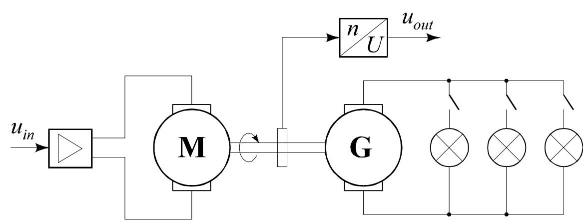

Fig. 22. Motor-generator laboratory set-up.

Fig. 23 shows the system time response when running the auto-tuning algorithm.

The process open-loop step response is shown in more details in Fig. 24. From the step response the following values of the process gain K_{PR}, and areas A_1 to A_5 were calculated by the auto-tuning algorithm: K_{PR}=0.7144, A_1=0.187, A_2=3.198·10^{-2}, A_3=4.357·10^{-3}, A_4=4.989·10^{-4}, A_5=4.881·10^{-5}, and the resulting PI and PID controller parameters are

$$\begin{aligned} &PI\text{:}\;\; K = 0.76,\; T_i = 0.136s \\ &PID\text{:}\;\; K = 3.14,\; T_i = 0.214s,\; T_d = 0.062s \end{aligned} \quad . \tag{52}$$

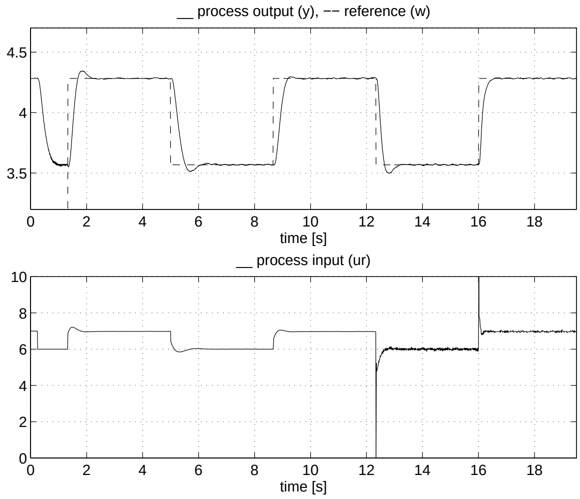

Fig. 23. Process output (upper Figure) and input (lower Figure) during the open-loop tuning period (0-1.3s) and the closed-loop testing period (1.3s-19s) of the auto-tuning algorithm.

The closed-loop responses (see Fig. 25) are very good for both controllers. It is obvious that the closed-loop response becomes faster when using PID controller. Different process transients at low and high reference levels again indicate the non-linear process characteristics.

Note that in this case also some noise at the process output is present.

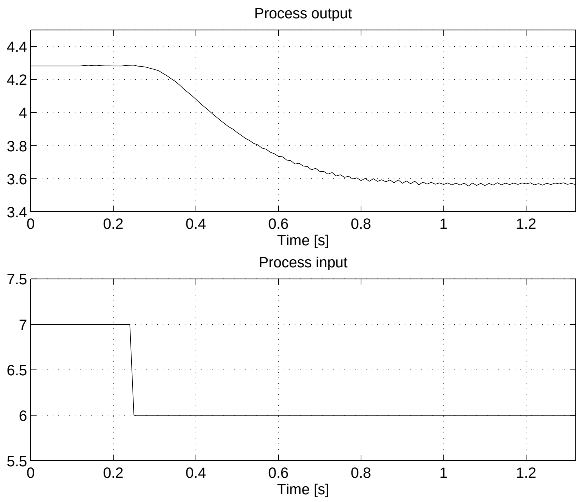

Fig. 24. The motor-generator set-up open-loop response.

5. DISCUSSION

The research related to the presented method was extended also to some other areas like e.g. multivariable PI controllers or Smith-predictor schemes. It was shown that the same idea with some modifications works quite successfully also in these domains (Vrančić et al., 1997b, Vrančić et al., 1998).

Unfortunately, the MOMI method has also some drawbacks which have to be mentioned.

Integration is a mathematical operation which is quite inert to moderate high frequency noise present in the process response. However, lower frequency noise, like disturbances in the measured system, can significantly deteriorate accuracy of the calculation of areas.

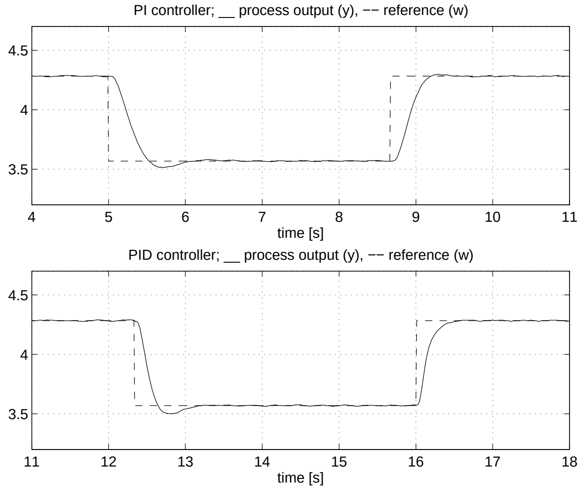

Fig. 25. The closed-loop process responses under PI and PID controller for the motor-generator set-up.

There are several different approaches to circumvent this problem. First, to use larger excitation signals at the process input if possible (since signal/disturbance ratio is higher, higher accuracy of the calculated areas can be obtained). Second, to carry out several different experiments on the process (the average of all process responses can then be used for the calculation of areas. This can significantly reduce the error, but on the other hand it also increases the time of experiment).

If neither the first nor the second approach is possible, the error in the calculation of controller parameters can be reduced by using lower number of areas. Namely, it is possible to calculate the PID controller parameters based only on three areas (instead of five), but such a solution is not more optimal according to the MO criterion, because the ratio T_d/T_i has to be fixed (Vrančić et al., 1997a). However, the obtained closed-loop responses of such a controller are still faster than those obtained by using the PI controller and are not oscillatory for majority of the process models which frequently appear in the process industry.

Beside the mentioned problems there are also some difficulties related to the drawbacks of the original magnitude optimum (MO) technique on which our approach is based. One of them is that the closed-loop stability is not guaranteed (Hanus, 1975). Namely, there exist processes with stronger zeros or complex poles, which correspond to equation (1), but give unstable controller parameters (Vrančić, 1997).

Even though it was not our prime intention to improve the original MO technique, some ways how to achieve stability for such processes by re-tuning controller parameters, were proposed (Vrančić, 1997).

Another, also frequently claimed problem is that the process poles are cancelled by the controller zeros. This may lead to poor attenuation of load disturbances if the cancelled poles are excited by disturbances, and if they are slow compared to the dominant closed-loop poles (Åström and Hägglund, 1995). Poorer disturbance rejection can be observed especially when controlling low-order processes. In such cases, disturbance rejection can be significantly improved by using a two-degrees-of-freedom PI (PID) controller (Vrančić, 1997).

We are planning to report about the results mentioned above in future publications.

6. CONCLUSIONS

The purpose of this lecture was to present a simple tuning method for the PI(D) controller, suitable for a large class of processes. The method is based on the magnitude optimum (frequency domain) criterion from which the formulae for calculation of PI(D) controller parameters are derived. These formulae are transformed into the new ones consisting mainly of different areas which can be calculated from the process step response by using the multiple integrations method. This results in a quite simple and straightforward time domain tuning approach. Simulation experiments on different kinds of processes have shown that the proposed method gives better results in comparison to some other, more frequently used, tuning procedures.

The method was also tested on two laboratory plants. It was shown that it is quite robust to the process high-frequency noise and non-linearity.

The drawback of this approach is that the method requires a stable open-loop process response in order to determine the appropriate controller parameters, and that the low-frequency noise or disturbances can significantly affect the accuracy of the calculated controller parameters if some additional precautions are not taken.

REFERENCES

Åström, K. J., T. Hägglund, C. C. Hang, and W. K. Ho (1993). Automatic Tuning and Adaptation for PID Controllers - A Survey. Control Engineering Practice, **1** (4), pp. 699-714.

Åström, K. J., and T. Hägglund (1995). PID Controllers: Theory, Design, and Tuning. *Instrument Society of America*, 2nd edition.

Gorez, R. (1997). A survey of PID Auto-Tuning Methods. Journal A, **38** (1), pp. 3-10.

Hanus, R. (1975). Determination of controllers parameters in the frequency domain. Journal A, **XVI** (3).

Kessler, C. (1955). Über die Vorausberechnung optimal abgestimmter Regelkreise Teil III. Die optimale Einstellung des Reglers nach dem Betragsoptimum. Regelungstechnik, Jahrg. **3**, pp. 40-49.

Nishikawa, Y., N. Sannomiya, T. Ohta, and H. Tanaka (1984). A Method for Auto-tuning of PID Control Parameters. Automatica, **20** (3), pp. 321-332.

Peng, Y., D. Vrančić, and R. Hanus (1996). Anti-windup, bumpless and conditioned transfer techniques for PID controllers, IEEE Control Systems Magazine, **16** (4), pp. 48-57.

Rake, H. (1987). Identification: Transient- and Frequency-Response Methods. Systems & Control Encyclopedia; Theory, Technology, Applications, Madan G Singh, ed., *Pergamon Press*.

Strejc, V. (1959). Näherungsverfrahren für aperiodische Übergangscharakteristiken. *Regelungstechnik 7*, pp. 124-128.

Umland, J. W., and M. Safiuddin (1990). Magnitude and Symmetric Optimum Criterion for the Design of Linear Control Systems: What Is It and How Does It Compare with the Others?. IEEE Transactions on Industry Applications, **26** (3), pp. 489-497.

Voda, A. A., and I. D. Landau (1995). A Method for the Auto-calibration of PID Controllers. Automatica, **31** (1), pp. 41-53.

Vrančić, D. (1997). Design of Anti-Windup and Bumpless Transfer Protection. *Doctoral thesis*.

Vrančić, D., Y. Peng, J. Petrovčič, and R. Hanus (1997a). A new tuning method for PID controllers. *Pre-prints of the 4th IFAC Conference on System Structure and Control*, Bucharest, pp. 438-443.

Vrančić, D., Y. Peng, J. Lieslehto, S. Strmčnik, and R. Hanus (1997b). Design of MIMO PI Controllers Using the Multiple Integration Approach. IMACS World Congress, Berlin, Vol. 5, pp. 149-154.

Vrančić, D., Y. Peng, and J. Petrovčič (1997c). A new simple auto-tuning method for PID controllers. *Pre-prints of the 2nd IFAC Workshop on New Trends in Design of Control Systems*, Smolenice, pp. 457-462.

Vrančić, D., R. Hanus, and S. Strmčnik (1998). A new tuning method for delayed processes based on the multiple integration method. *Accepted by the IFAC Conference on System Structure and Control,* Nantes, July 8-10, 1998.

Ziegler, J. G., and N. B. Nichols (1942). Optimum settings for automatic controllers. Trans. ASME, **64**, pp. 759-768.